

Percolation, relaxation halt, and retarded van der Waals interaction in dilute systems of iron nanoparticles

R. V. Chamberlin, Joachim Hemberger, Alois Loidl, K. D. Humfeld, D. Farrell, S. Yamamuro, Y. Ijiri, S. A. Majetich

Angaben zur Veröffentlichung / Publication details:

Chamberlin, R. V., Joachim Hemberger, Alois Loidl, K. D. Humfeld, D. Farrell, S. Yamamuro, Y. Ijiri, and S. A. Majetich. 2002. "Percolation, relaxation halt, and retarded van der Waals interaction in dilute systems of iron nanoparticles." *Physical Review B* 66 (17): 172403.
<https://doi.org/10.1103/PhysRevB.66.172403>.



Percolation, relaxation halt, and retarded van der Waals interaction in dilute systems of iron nanoparticles

R. V. Chamberlin,* J. Hemberger, and A. Loidl

Experimentalphysik V, Institut für Physik, Universität Augsburg, D-86135 Augsburg, Germany

K. D. Humfeld, D. Farrell, S. Yamamuro, Y. Ijiri,[†] and S. A. Majetich

Physics Department, Carnegie Mellon University, Pittsburgh, Pennsylvania 15213-3890

(Received 5 March 2002; published 11 November 2002)

We find three unanticipated features in the magnetic response of dilute systems of highly monodisperse Fe nanoparticles. Above a spin freezing temperature (T_f) the remanent magnetization relaxes smoothly to zero, but below T_f the relaxation halts abruptly at a nonzero value. The distribution of relaxation rates changes at a percolation temperature (T_p), consistent with chainlike structures above T_p and three-dimensional clusters below T_p . The blocking temperature (T_b) varies inversely proportional to particle diameter, opposite to the behavior of the Néel-Brown model for individual domains, but consistent with a type of Casimir-Polder interaction expected between dilute nanometer-scale particles.

DOI: 10.1103/PhysRevB.66.172403

PACS number(s): 75.75.+a, 34.30.+h, 61.46.+w, 75.60.Lr

Systems of magnetic nanoparticles have received considerable attention in recent years, partly for potential applications in high-density magnetic recording,¹ but also for exotic behaviors such as macroscopic tunneling² and quantum computing.³ Here we investigate magnetic interactions on nanoscopic length scales, intermediate between local quantum exchange and long-ranged dipolar interactions. The dynamic response of systems of highly dilute and monodisperse Fe nanoparticles reveals some intriguing phenomena that depend on the temperature regime. One observation is an abrupt halt in the relaxation at long times and low temperatures, which we attribute to the dipolar interaction in clusters that contain a sufficient number of particles. Another feature is a maximum in the effective width of the relaxation spectrum, indicative of a type of percolation transition. Furthermore, the blocking temperature exhibits an *inverse* diameter dependence, which may be attributed to the Casimir-Polder mechanism^{4,5} for a van der Waals (vdW) interaction between particles that is retarded by the finite speed of light. The retarded vdW force has previously been measured between various small objects,⁶⁻⁹ and has recently been predicted to result in a magnetic coupling between parallel plates.¹⁰ Here we present evidence for similar long-ranged quantum effects inside a bulk assemblage of ferromagnetic nanoparticles.

Three different sets of Fe particles were used for this study. The samples had mean particle diameters of $d=5.5$, 7.2, and 8.0 nm, with a full width at half maximum of 1.1, 1.3, and 1.2 nm, respectively. The nanoparticles were prepared by thermal decomposition of iron pentacarbonyl in dioctyl ether as described previously,^{11,12} then diluted to 0.1 vol %, which yields an average separation between particles of $D \approx 10d$. To minimize oxidation, the samples were sealed under argon in glass ampoules. Temperature-dependent measurements of zero-field cooled (ZFC) and field-cooled (FC) magnetization were made using a Quantum Design MPMSXL magnetometer. Time-dependent magnetic response was obtained using a special-purpose superconducting quantum interference device (SQUID) magnetometer

that is optimized for measuring magnetic relaxation in a single sweep from 10^{-5} – 10^4 s after removing an applied field.

Figure 1 shows the ZFC and FC magnetizations for two of the samples. We identify the blocking temperature (T_b) with the maximum in the ZFC curve; other ways of defining T_b do not significantly alter our conclusions. The measured values, $T_b(5.5)=42.6$, $T_b(7.2)=30.2$, and $T_b(8.0)=28.6$ K, are consistent with an inverse diameter dependence, $T_b \approx 230 \text{ K} / (d/\text{nm})$. The higher T_b for smaller particles is opposite to the behavior expected from classical models of individual domain rotation,^{13,14} emphasizing the importance of interparticle interactions.^{15,16}

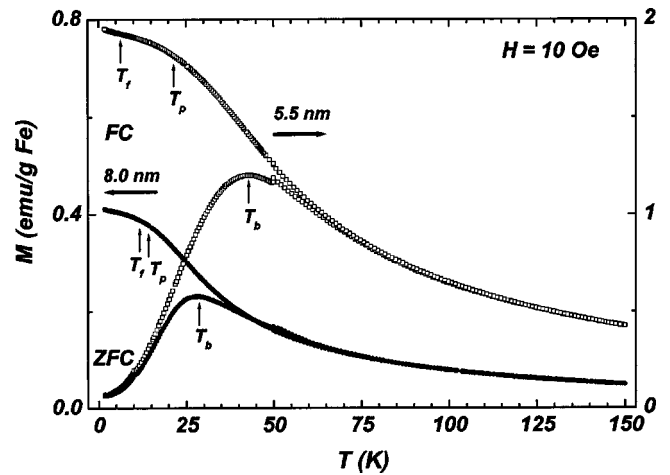


FIG. 1. Zero-field cooled (ZFC) and field cooled (FC) magnetization as a function of temperature from the samples containing 5.5-nm (open squares and right axis) and 8.0-nm (solid circles and left axis) Fe particles. The blocking temperatures, as defined by the maximum in the ZFC magnetization, are $T_b(5.5)=42.6$ and $T_b(8.0)=28.6$ K. The percolation temperatures, as defined by the maximum amount of curvature in the FC curves, are $T_p(5.5)=21.4$ and $T_p(8.0)=14.5$ K. The freezing temperatures, as found from the dynamics shown in Fig. 2, are $T_f(5.5)=6$ and $T_f(8.0)=12$ K.

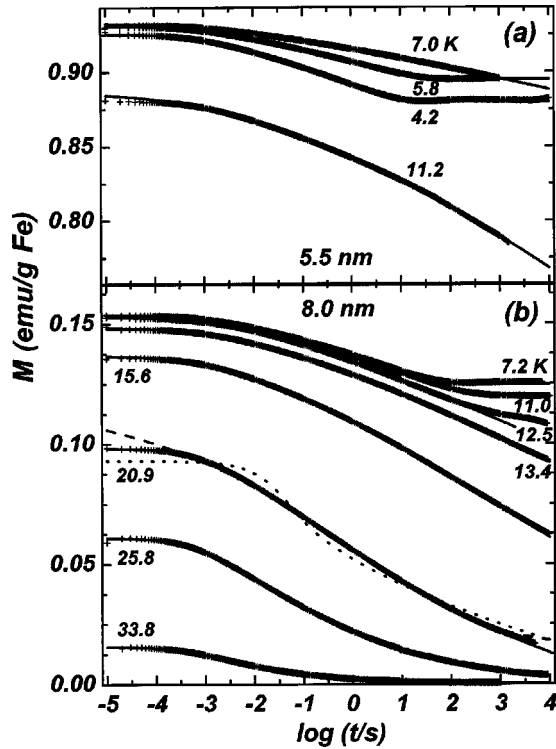


FIG. 2. Semilog plot of magnetic remanence as a function of time after removing a field of 4 Oe, at several temperatures, for the samples containing (a) 5.5-nm and (b) 8.0-nm Fe particles. The solid curves are best fits to the data using Eq. (3), with the 1D percolation distribution above 15 K, and the 3D distribution of finite clusters with $p > p_c$ below 15 K. The dotted and dashed curves in (b) are a best fit to the 20.9-K data using the 3D distribution with $p < p_c$ and stretched exponential function, respectively. Below a freezing temperature [$T_f(5.5) = 6$ K and $T_f(8.0) = 12$ K], the relaxation exhibits an abrupt halt and permanent remanence after a freezing time [$t_f(5.5) = 20$ s and $t_f(8.0) = 100$ s]. The halt can be characterized by including a cutoff in the maximum cluster size in Eq. (3), as shown by the solid curves fitted to the 4.2- and 5.8-K data in (a), and the 7.2- and 11.0-K data in (b).

Magnetic relaxation was measured as follows. First the sample was heated to 45 K (where the response is rapid) and a field of 4 Oe was applied. Next the sample was field cooled to the measurement temperature, where it was held for 4 min to allow the temperature to stabilize. Then the field was removed, and the magnetization measured at 10 μ s intervals for the first 1 ms, and at increasing intervals until 200–10 000 s. Figure 2 is a plot of the remanent magnetization versus logarithm of time at several temperatures for two of the samples. Figure 2(b), for the 8.0-nm sample, shows that some relaxation remains on the ms time scale well above T_b . The relaxation slows down gradually with decreasing temperature until about 13 K where the relaxation extends across the entire time window of our magnetometer, with no evidence for a permanent remanence at long times.

The most striking feature in the dynamics is an abrupt halt in the relaxation after a freezing time t_f below a freezing temperature T_f . From Fig. 2(a) we find $t_f(5.5) = 20$ s and $T_f(5.5) = 6$ K; and from Fig. 2(b) $t_f(8.0) = 100$ s and $T_f(8.0) = 12$ K. Thus, in contrast to T_b which decreases with

increasing particle diameter, T_f increases with increasing diameter. Although it is possible that the freezing occurs inside individual particles, it is difficult to imagine how such internal freezing could halt the dynamics at long times without influencing the faster dynamics that occurs over the first 6–7 orders of magnitude in our time window. Furthermore, it is known that the primary response of even bulk Fe occurs on the ms time scale throughout this temperature regime.¹⁷ Thus the evidence indicates that the dynamical freezing is also due to interparticle interactions.

First we consider the magnetic dipole interaction between two spherical particles of diameter d with distance r between their centers. The average interaction energy, from the thermal average over all orientations at temperature T ,¹⁸ is $u(T, r) = (-1/kT)2\mu_1^4/3r^6$. Here μ_1 is the net magnetic moment of each particle, which using bulk values for the Fe density and saturated magnetic moment gives $\mu_1/\mu_B = 9.9 \times 10^{22} d^3$, where μ_B is the Bohr magneton. The total interaction energy for a typical particle is found by integrating $u(T, r)$ over all $r \geq d$, weighted by the probability [$\eta(r)dr$] of finding a neighboring particle in a spherical shell of thickness dr . The particles are suspended in a nonmagnetic fluid which freezes at ~ 200 K as the sample is first cooled. Because the interaction energy between most particles is much less than the thermal energy when the fluid freezes, the frozen-in positions of the particles should be essentially random, yielding a constant density of particles, and $\eta(r)dr \approx 4\pi r^2 dr / [(4\pi/3)D^3]$. Now integrating over $r \geq d$, the interaction energy per particle becomes $u(T) = (-1/kT)2\mu_1^4/(Dd)^3$. An estimate for the temperature where the dipole alignments freeze, $|u|/k$, is obtained by equating $|u(T)|$ to the thermal energy. For the 0.1 vol% samples we find

$$|u|/k = 0.27 \text{ K } (d/\text{nm})^3, \quad (1)$$

which varies from 45 to 140 K for the 5.5–8.0-nm samples, respectively. Although the order of magnitude of $|u|/k$ is similar to the measured blocking temperatures, the size dependence is opposite from that of T_b , suggesting that the dipolar freezing should be associated with the relaxation halt. The quantitative difference between $|u|/k$ and T_f can be attributed to the reduced density and magnetic moment of small particles compared to the bulk values of Fe, combined with internal thermal fluctuations¹⁹ which further reduce the magnetic moment below that of a saturated particle. Indeed, cooperative effects due to the mutual interaction between many particles may cause an abrupt freezing, as is observed at T_f . Furthermore, because the dipole interaction is long ranged, small clusters of particles may avoid this freezing and continue to relax when $T < T_f$, as is also observed.

van der Waals forces exist between all objects that contain electrical charge. Retardation effects arise from the non-negligible time delay for information to travel between the objects when their separation exceeds a few nanometers. The interaction is usually only relevant for objects with no permanent dipole. However, such long-ranged quantum effects may be important on intermediate length scales due to the relatively weak magnetostatic interaction, somewhat like the

exchange interaction dominating over dipolar effects inside bulk ferromagnets. A general expression for the retarded vdW interaction energy between two spheres of diameter d and separation r is $\nu(r) = -P\hbar c d^6/r^7$. Here $2\pi\hbar$ is Planck's constant, c is the speed of light, and P is a dimensionless constant that depends on the fluctuations induced in the two objects. The average interaction energy is found by integrating $\nu(r)$ over all $r \geq d$, weighted by $\eta(r)dr$, yielding $\nu \approx -3P\hbar c d^2/4D^3$. Thus, for any system with $D \propto d$, the retarded vdW interaction gives $\nu \propto -1/d$. Specifically, for our samples with $D \approx 10d$, assuming solid conducting spheres of radius $(d/2)$, including electric and magnetic interactions to second order²⁰ yields $P = [143/16 + 1/3(1631/48 - 8839/960)][(1/2)^6/\pi]$, and

$$|\nu|/k = 147 \text{ K} / (d/\text{nm}). \quad (2)$$

Equation (2) gives the qualitative inverse diameter dependence, and is within a factor of 2 of the measured blocking temperatures. However, a key assumption needs to be verified. We have assumed that the vdW-like electron fluctuations couple strongly to the magnetic alignment, which is not valid if the spin-orbit coupling is too weak. Similarly, a spin-specific component for the Casimir effect¹⁰ may also be too weak. Nevertheless, the $1/r^7$ dependence yields much stronger than average interactions between very close particles; and even if the particles are touching, $D \approx d$ in the retarded vdW interaction still gives $\nu \propto -1/d$. Further evidence for this nonclassical interaction on intermediate length scales comes from a detailed analysis of the magnetic relaxation.

The dashed curve in Fig. 2 is a best fit to the 20.9-K data using the stretched exponential function showing that this standard relaxation formula does not adequately describe the data. The solid curves are from a percolation model for random clusters of interacting particles. The model is adapted from an earlier model²¹ by utilizing the one-dimensional (1D) distribution of clusters at high temperatures, and by having an activation energy that is *proportional* to cluster size. [Note "size" refers to the number of particles (m) in the cluster, which is proportional to volume.] In contrast, activation energies for clusters inside many materials vary *inversely* proportional to size,²² and Eq. (2) varies inversely proportional to particle diameter. Here, however, all particles in each sample have essentially the same size, so that the average activation energy increases smoothly with m . If E_0 is the activation energy per particle, with w_0 a fundamental relaxation rate, the relaxation rate of a cluster of m particles is $w_m = w_0 \exp[-mE_0/kT]$. Assuming linear and extensive cluster response, with a distribution of cluster sizes g_m , the time-dependent magnetization is $M(t) \propto \sum_{m=1}^{\infty} m g_m e^{-t w_m}$. Converting this sum to an integral, and making a change in the dummy variable of integration to x ($\propto m$), the function we use to fit data is

$$M(t) = M_0 \int_0^{\infty} x g_x e^{-t w_x} dx, \quad (3)$$

where g_x is the scaled distribution of cluster sizes and $w_x = w_0 \exp[-Cx]$ gives their relaxation rates. The adjustable parameters in Eq. (3) are: M_0 for the amplitude of response,

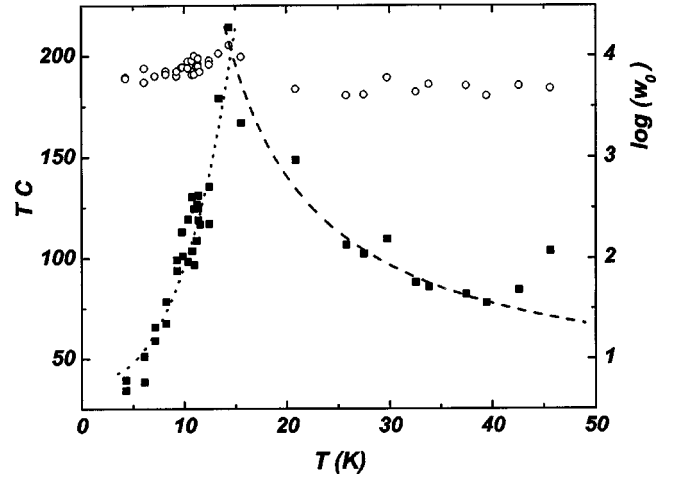


FIG. 3. Temperature dependence of two of the parameters obtained from best fits to the magnetic relaxation of the sample containing 8.0-nm Fe particles. The fundamental relaxation rate (open circles and right scale) is roughly constant at $w_0 = 6,800 \text{ s}^{-1}$. The product of temperature times correlation coefficient (solid squares and left scale), from TC_1 above 15 K and TC_3 below 15 K, shows a peak at $T_p \approx 15 \text{ K}$. The dashed curve is proportional to $1/|\ln p|$, and the dotted curve is proportional to $1/(p-p_c)^{2.2}$, using $p_c = 0.3$ and $p = 1 - \exp(-T_p/T)$.

w_0 for the time scale of relaxation, and the correlation coefficient C for the width and shape of the response. A constant offset is added to Eq. (3) to adjust for small uncertainties in the measured zero point of the magnetization. With the same number of parameters as the stretched exponential, Eq. (3) gives significantly better agreement with the data.

Generally good agreement with all measured relaxation is obtained using the 3D percolation distribution with a correlation probability that is greater than the critical probability $p > p_c$,²³ $g_x \propto x^{1/9} \exp(-x^{2/3})$. However, above a percolation temperature, $T_p(8.0) \approx 15 \text{ K}$, small but consistent improvement is achieved using the 1D distribution, $g_x \propto \exp(-x)$. Although the differences between the $p > p_c$ 3D and $p < p_c$ 1D distributions are difficult to see on the scale of Fig. 2, the dotted curve fitted to the 20.9-K data using $g_x \propto x^{-3/2} \exp(-x)$ shows that the response clearly deviates from the $p < p_c$ 3D distribution. The relaxation halt at long times and low temperatures can be empirically characterized by inserting a sharp cutoff for the upper limit of integration (x_c instead of ∞) in Eq. (3), as shown by the solid curves fitted to the two lowest temperatures for each sample. The cutoff values are $x_c(5.5) = 1.76 \pm 0.07$ and $x_c(8.0) = 1.36 \pm 0.09$, but x is a dummy variable of integration so the actual number of particles at the cutoff is unclear. A relaxation halt for $x > x_c$ is consistent with the dipolar interaction, which dominates at large distances and may abruptly increase the activation barrier of large clusters. Although both the time and temperature dependence of the relaxation halt are suggestive of the dipolar interaction, further studies are necessary to confirm this interpretation.

Figure 3 shows that there is little or no temperature dependence of the fundamental relaxation rate for the 8.0-nm sample. Its value ($w_0 = 6800 \text{ s}^{-1}$) is similar to the relaxation

rate of bulk Fe over the same range,¹⁷ consistent with the model that w_0 corresponds to the reorientation rate of each nanoparticle. Also shown in Fig. 3 is the product of temperature times correlation coefficient TC . The peak in TC at $T_p(8.0) \approx 15$ K suggests a type of percolation transition, but because the change is from one dimension to three dimensions, it is not the usual percolation on a homogeneous distribution of particles with fixed interactions. A possible explanation comes from the rapid ($1/r^7$) drop off in the interaction between particles. At high temperatures, a significant probability of correlation occurs only between a particle and its one or two nearest neighbors, forming quasi-1D chains. With decreasing temperature, the range of correlation increases, until at T_p the 1D chains couple into 3D clusters. Support for this picture comes from measurements of T_p as a function of sample dilution. For homogeneous interactions, T_p would vary proportional to the vol% of nanoparticles. Instead we find that T_p varies like the cube root of vol%, indicative of quasi-1D behavior.

The temperature dependence of the percolation behavior can be characterized by using a standard thermal function for the probability that two neighbors are strongly correlated, $p = 1 - \exp(-T_p/T)$. Via the change of variables, percolation theory predicts $TC_1 \propto E_0/|\ln p|$ above T_p and $TC_3 \propto E_0/(p - p_c)^{2.2}$ below T_p . The dashed and dotted curves in Fig. 3 show reasonable agreement with the data using a sensible value of $p_c = 0.3$, with an amplitude factor for each function as the only adjustable parameters. This analysis indicates that the sample is heading towards a percolation transition as T_p is approached from either side, but the transition is interrupted by a dimensional crossover. Evidence for the crossover also appears in Fig. 1, where there is a maximum in the amount of curvature in the FC magnetization at a similar temperature. From the third derivative of a fourth-order fit to the FC curves we obtain $T_p(5.5) = 21.4$ and $T_p(8.0) = 14.5$ K, giving $T_p \approx 120$ K/(d/nm), within about 20% of Eq. (2). However, measurements as a function of particle dilution emphasize that the actual situation is not so simple;

the average interaction energy between randomly located neighbors does not adequately describe the net behavior. Nevertheless, from the measured values of T_f and T_b , we estimate that the limit on Fe particle diameters in a 0.1 vol% sample for the retarded vdW interaction to exceed the dipolar interaction is $d < 10$ nm.

In summary, we have found several unanticipated features in the magnetic response of systems of dilute Fe nanoparticles. The blocking temperature varies inversely proportional to particle diameter, indicating that T_b is governed by interparticle separation, not particle size. Despite the narrow distribution of particle sizes, the spectrum of magnetic relaxation at low temperatures is very broad, consistent with a percolation model for clusters having relaxation times that increase exponentially with the number of particles in each cluster. The maximum spectral width occurs at a type of percolation crossover from 1D chains above T_p to 3D clusters below T_p . Below a sharp freezing temperature the remanent magnetization relaxes for at least 6 orders of magnitude in time, then halts abruptly on a time scale that increases with increasing particle size. We associate the freezing at T_f with the magnetic-dipole interaction between particles; whereas both T_p and T_b vary inversely proportional to particle diameter, consistent with the Casimir-Polder type of retarded van der Waals interaction expected between conducting spheres. Thus all prominent features in the slow magnetic response can be attributed to interparticle interactions, and long-ranged quantum effects may be important in many systems on nanometer length scales.

We thank P. Bruno and D. C. Prieve for discussions, and the National Science Foundation for support of this research through Grant Nos. DMR-9701740 (R.V.C.) and DMR-9900550 (S.A.M.). R.V.C. also thanks A. Loidl and his group for their hospitality and the Alexander von Humboldt Foundation for support while in Augsburg, Germany. Additional support was provided by the bmb+f/VDI through Contract No. EKM 13N6917-A.

*Permanent address: Department of Physics and Astronomy, Arizona State University, Tempe, AZ 85287-1504.

†Permanent address: Department of Physics, Oberlin College, Oberlin, OH 44074.

¹D. E. Speliotis, J. Magn. Magn. Mater. **193**, 29 (1999).

²L. Thomas, F. Lioni, R. Ballou, D. Gatteschi, R. Sessoli, and B. Barbara, Nature (London) **383**, 145 (1996).

³M. N. Leuenberger and D. Loss, Nature (London) **410**, 789 (2001).

⁴H. B. G. Casimir and D. Polder, Phys. Rev. **73**, 360 (1948).

⁵E. Elizalde and A. Romeo, Am. J. Phys. **59**, 711 (1991).

⁶D. Tabor and R. H. S. Winterton, Nature (London) **219**, 1120 (1968).

⁷U. Mohideen and A. Roy, Phys. Rev. Lett. **81**, 4549 (1998).

⁸X. Wu and T. G. M. van de Ven, Langmuir **12**, 6291 (1996).

⁹M. A. Bevan and D. C. Prieve, Langmuir **15**, 7925 (1999).

¹⁰P. Bruno, Phys. Rev. Lett. **88**, 240401 (2002).

¹¹K. D. Humfeld, A. K. Giri, S. A. Majetich, and E. L. Venturini, IEEE Trans. Magn. **37**, 2194 (2001).

¹²R. V. Chamberlin, K. D. Humfeld, D. Farrell, S. Yamamuro, Y. Ijiri, and S. A. Majetich, J. Appl. Phys. **91**, 6961 (2002).

¹³L. Néel, Ann. Geophys. **5**, 99 (1949).

¹⁴W. F. Brown, Phys. Rev. **130**, 1677 (1963).

¹⁵M. F. Hansen and S. Mørup, J. Magn. Magn. Mater. **184**, 262 (1998).

¹⁶J. L. Dormann, D. Fiorani, and E. Tronc, J. Magn. Magn. Mater. **202**, 251 (1999).

¹⁷R. V. Chamberlin and M. R. Scheinfein, Science **260**, 1098 (1993).

¹⁸C. E. Hecht, *Statistical Thermodynamics and Kinetic Theory* (Freeman, New York, 1990).

¹⁹S. N. Khanna and S. Lindroth, Phys. Rev. Lett. **67**, 742 (1991).

²⁰G. Feinberg, Phys. Rev. B **9**, 2490 (1974).

²¹R. V. Chamberlin and D. N. Haines, Phys. Rev. Lett. **65**, 2197 (1990).

²²R. V. Chamberlin, Phase Transitions **65**, 169 (1998).

²³D. Stauffer, *Introduction to Percolation Theory* (Taylor and Francis, London, 1985).